Contemporary Mathematics
http://ojs.wiserpub.com/index.php/CM/

Research Article

A Fractional-Order Mathematical Model of Banana Xanthomonas Wilt Disease Using Caputo Derivatives

A. Manickam[1*], M. Kavitha[2], A. Benevatho Jaison[1], Arvind Kumar Singh[3]

[1]Mathematics Division, School of Advanced Sciences and Languages, VIT Bhopal University, Bhopal-Indore Highway, Kothrikalan, Sehore, Madhya Pradesh - 466114, India
[2]Department of Mathematics, Panimalar Engineering College, Chennai-600123, Tamil Nadu, India
[3]Department of Mathematics, Institute of Science, Banaras Hindu University, Varanasi-221005, Uttar Pradesh, India
E-mail: manickammaths2011@gmail.com

Received: 11 February 2023; **Revised:** 7 March 2023; **Accepted:** 5 April 2023

Abstract: This article investigates a fractional-order mathematical model of Banana Xanthomonas Wilt disease while considering control measures using Caputo derivatives. The proposed model is numerically solved using the L1-based predictor-corrector method to explore the model's dynamics in a particular time range. Stability and error analyses are performed to justify the efficiency of the scheme. The non-local nature of the Caputo fractional derivative, which includes memory effects in the system, is the main motivation for incorporating this derivative in the model. We obtain varieties in the model dynamics while checking various fractional order values.

***Keywords*:** mathematical model, Caputo fractional derivative, L1 predictor-corrector scheme, error analysis, stability, graphical simulations

MSC: 26A33, 34C60, 65D05, 65L07

1. Introduction

Banana Xanthomonas Wilt (BXW), a destructive bacterial disease caused by a bacterium called *Xanthomonas campestris* pv. *musacearum* (Xcm), has been identified as the major disease that threatens banana farming in East Africa [1]. The vectors, like bats, birds, and flying insects (e.g., bees), spread the Xcm bacteria from an infected banana plant to a susceptible banana plant. The long-distance spread of Xcm is mainly caused by birds and bats [2]. The common symptoms of BXW are yellowing and withering of leaves, untimely ripening and rotting of the fruit, shriveling and blackening of male gusset bloom, yellow drip presented on the cross-cut of the banana plant pseudo-trunk, and lastly, plant death [3, 4]. The authors in [5] observed community mobilization as a key to controlling BXW disease management. In [6], the authors analyzed the possibilities of removing the infected plant and leaving the uninfected plant to grow. The authors in [7] also investigated that time-to-time removing the infected plants from the mat is the best control compared to removing the complete mat, which is costly, time-consuming, and requires more labor. In [8], the authors explored BXW control techniques in Rwanda.

Several mathematical models have been derived by researchers to understand the transmission dynamics of BXW disease and provide possible control techniques. In [9], the authors derived a model to understand the transmission

DOI: https://doi.org/10.37256/cm.5120242479

structure of the BXW epidemic by vectors with control measures. In [10], the authors proposed a non-linear model to analyze the role of contaminated measures in the reiteration of BXW. In [11], the researchers proposed a model considering roguing and debudding controls for the BXW transmission. Nakakawa et al. [12] considered the vertical and vector mode transmissions in the BXW dynamical model. Kweyunga et al. [13] developed a model of BXW considering both horizontal and vertical modes of transmission. In [14], the authors derived a non-linear model to analyze the role of neglected control measures in the BXW transmission.

Nowadays, fractional calculus [15-17] is being applied to solve various real-world problems in terms of mathematical modeling. Different types of fractional derivatives [18, 19] have been successfully used to model various problems. More specifically, several deadly epidemics have been modeled by using mathematical models in a fractional-order sense. It is a well-known fact that fractional-order operators are non-local in nature and may be more effective for modeling history-dependent systems. Moreover, a fractional order can be fixed as any positive real number that better fits the real data. So, by using such an operator, an accurate adjustment can be made in a model to fit with real data for better predicting the outbreaks of an epidemic. Recently, several applications of fractional derivatives have been recorded in epidemiology. In [20-25], the authors have studied the dynamics of the COVID-19 disease by using fractional-order models. In [26], the authors proposed the mathematical modeling of typhoid fever in terms of fractional-order operators. In [27], a fractional-order model of the Chlamydia disease is proposed. In [28], the dynamics of the Chagas-HIV epidemic model using various fractional operators are explored. In [29], the authors derived a novel non-linear model for the dynamics of tooth cavities in the human population. In [30], the authors performed an analysis of the stability and bifurcation of a delay-type fractional-order model of HIV-1. In [31], the authors solved a fractional-order HIV-1 infection of CD4+ T-cells considering the impact of antiviral drug treatment. In [32], the authors defined a fractal-fractional model of the AH1N1/09 virus. In [33], the authors studied the dynamics of a fractional-order host-parasitoid population model describing insect species. In [34], the authors used a wavelet-based numerical method for a fractional-order model of measles using Genocchi polynomials. In [35], some theoretical analyses of the Caputo-Fabrizio fractional-order model for hearing loss due to the mumps virus with optimal controls were proposed.

Several numerical methods have been proposed by researchers to solve fractional-order problems. In [36], the authors derived a new generalized form of the predictor-corrector (PC) scheme to investigate fractional initial value problems (IVPs). Kumar et al. [37] introduced a new method to simulate fractional-order systems with various examples. In [38], the PC method was derived to simulate delayed fractional differential equations. A modified form of the PC scheme in terms of the generalized Caputo derivative to solve delay-type systems has been introduced in [39]. Odibat et al. [40] have derived the generalized differential transform method for solving fractional impulsive differential equations. The authors in [41] introduced a novel finite-difference predictor-corrector (L1-PC) scheme to solve fractional-order systems in the sense of the Caputo derivative. In [42], the authors proposed a new form of L1-PC scheme to solve multiple delay-type fractional-order systems. In [43], a novel numerical scheme to solve fractional differential equations in terms of Caputo-Fabrizio derivatives was proposed. In [44], the authors derived a difference scheme for the time fractional diffusion equations. In [45], a second-order scheme for the fast evaluation of the Caputo-type fractional diffusion equations has been derived. In [46], the authors defined a fractional clique collocation method for numerically solving the fractional Brusselator chemical model. In [47], the researchers derived efficient matrix techniques for solving the fractional Lotka-Volterra population model.

To date, the aforementioned studies of mathematical modeling of the BXW disease [9-14] have yet to be analyzed using fractional derivatives. In this paper, we generalize the non-linear control-based model of BXW [14] by using Caputo fractional derivatives. The motivation behind this generalization is that fractional derivatives are non-local and may be more effective to include memory effects in the model.

The rest of this paper is designed as follows: In Section 2, some preliminaries are recalled. The model description in the Caputo sense is given in Section 3. The numerical analysis containing the solution algorithm, error estimation, and stability are given in Section 4. The graphical simulations are performed in Section 5. Concluding remarks are given in Section 6.

2. Preliminaries

The preliminaries are as follows:

Definition 1. A function (real) $f(s)$, $s > 0$ belongs to the space

(a) $C_\eta, \eta \in \mathbb{R}$ if there exists a real number $q > \eta$, such that $f(s) = s^q f_1(s), f_1 \in C[0, \infty)$. Therefore, $C_\eta \subset C_\alpha$ if $\alpha \le \eta$.

(b) $C_\eta^m, m \in \mathbb{N} \cup \{0\}$ if $f^{(m)} \in C_\eta$.

Definition 2. [16] The Riemann-Liouville (R-L) fractional integral of $f(t) \in C_\eta \left(\eta \ge -1\right)$ is defined as follows:

$$J^\omega f(t) = \frac{1}{\Gamma(\omega)} \int_0^t (t-s)^{\omega-1} f(s) ds,$$

$$J^0 f(t) = f(t).$$

Definition 3. [16] The R-L fractional derivative of $f \in C_-^m$ is given by

$$^{RL}D_t^\omega f\left(t\right) = \left(\frac{d}{dt}\right)^m \frac{1}{\Gamma(m-\omega)} \int_0^t (t-\xi)^{m-\omega-1} f(\xi) d\xi,$$

where $m = [\omega] + 1$ and $[\omega]$ are the integer-part of ω.

Definition 4. [16] The Caputo fractional derivative of $f \in C_{-1}^m$ is given by

$$^C D_t^\omega f\left(t\right) = \begin{cases} \dfrac{d^m f\left(t\right)}{dt^m}, & \text{if } \omega = m \in \mathbb{N}, \\ \dfrac{1}{\Gamma(m-\omega)} \displaystyle\int_0^t \left(t-\vartheta\right)^{m-\omega-1} f^{(m)}\left(\vartheta\right) d\vartheta, & \text{if } m-1 < \omega \le m, m \in \mathbb{N}. \end{cases} \tag{1}$$

Remark 1. The most common difference between the R-L and Caputo fractional derivatives is that the R-L derivative problems contain fractional initial conditions, whereas Caputo's definition uses classical conditions. Also, the derivative of a constant function is zero by the Caputo derivative but not by the R-L definition.

3. Model description

Here, we define the Caputo-type fractional-order generalization of a BXW disease model, including some control measures, which was given in [14]. We know that fractional derivatives are non-local differential operators that allow memory effects in the system, which is a very important feature for studying disease outbreaks more accurately. The model contains two population sizes: the banana population (N_p) and the insect vector population (N_v). The population of banana plants involves three different classes: susceptible plants (S_p), asymptomatic infectious plants (A_p), and symptomatic infected plants (I_p). The population of vectors involves two classes: susceptible vectors (S_v) and vectors contaminated with Xcm bacteria (I_v). An environment contaminated with Xcm bacteria is defined by E_b. The model is given as follows:

$$\begin{aligned}
&^C D^\omega S_p = b_p^\omega - (1-\xi)\Big(a^\omega \gamma_1 \frac{S_p I_v}{N_p} + \beta_a^\omega \frac{S_p A_p}{N_p} + \beta_s^\omega \frac{S_p I_p}{N_p} + \gamma_2 \frac{S_p E_b}{N_p (K + E_b)}\Big) - \alpha_p^\omega S_p, \\
&^C D^\omega A_p = (1-\xi)\Big(a^\omega \gamma_1 \frac{S_p I_v}{N_p} + \beta_a^\omega \frac{S_p A_p}{N_p} + \beta_s^\omega \frac{S_p I_p}{N_p} + \gamma_2 \frac{S_p E_b}{N_p (K + E_b)}\Big) + (1-\delta)\theta^\omega I_p - (\alpha_p^\omega + q^\omega) A_p, \\
&^C D^\omega I_p = q^\omega A_p - (\alpha_p^\omega + d^\omega + r^\omega) I_p, CD^\omega E_b = \phi^\omega I_p - (\mu_b^\omega + \psi) E_b, \\
&^C D^\omega S_v = b_v^\omega + \eta^\omega I_v - a^\omega \gamma_3 \frac{S_v I_p}{N_p} - \mu_v^\omega S_v, \\
&^C D^\omega I_v = a^\omega \gamma_3 \frac{S_v I_p}{N_p} - (\eta^\omega + \mu_v^\omega) I_v,
\end{aligned} \tag{2}$$

with the initial conditions

$$S_p(0) > 0, A_p(0) \geq 0, I_p(0) \geq 0, E_b(0) \geq 0, S_v(0) > 0, I_v(0) \geq 0, \tag{3}$$

where ${}^C D^{\omega}$ is the Caputo fractional derivative operator of order ω. For setting the same dimensions $t^{-\omega}$ at both sides of the fractional-order model, we applied the power ω on the parameters, those are in time unit t^{-1}.

The compartmental diagram of the model is given in Figure 1.

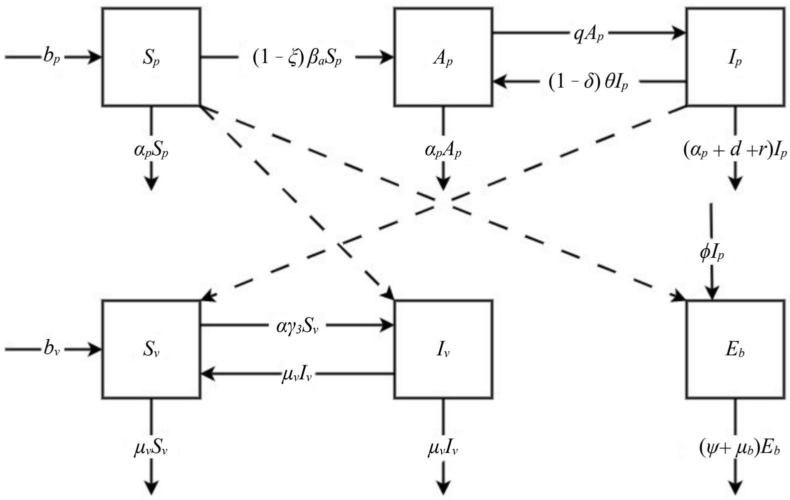

Figure 1. Compartmental diagram of the model

The variations in the population size $N_p = S_p + A_p + I_p$, and $N_v = S_v + I_v$ are defined as follows:

$$\begin{aligned} {}^C D^{\omega} N_p &= b_p^{\omega} - \alpha_p^{\omega} N_p + (1-\delta)\theta^{\omega} I_p - (d^{\omega} + r^{\omega}) I_p, \\ {}^C D^{\omega} N_v &= b_v^{\omega} - \mu_v^{\omega} N_v. \end{aligned} \tag{4}$$

The model parameters with numerical values are defined in Table 1.

Table 1. Parameters with numerical values [14]

Parameter	Identification	Values
b_p	Rate of recruitment of susceptible suckers	0.01667
b_v	Birth rate of susceptible vectors	0.02
α_p	Rate of harvesting of old plants	0.0056
θ	Vertical transmission rate from an infected plant	0.0286
r	Removal rate of infected plant	0.5
d	Death rate caused by BXW	0.0167
β_a	Rate of infection caused by contaminated farming measures from asymptomatic infected plants	0.3
β_s	Rate of infection caused by contaminated farming measures from symptomatic infected plants	0.1429
a	Contact rate between vectors and banana plants	0.2
γ_1	Probability of Xcm bacteria transmission from an infected vector to a susceptible plant when in contact	0.2
γ_2	Probability of Xcm bacteria transmission from contaminated soil to a susceptible plant	0.4
γ_3	Probability of Xcm bacteria transmission from an infected plant to a susceptible vector	0.2
μ_v	Death rate of the vectors	0.02
η	Rate of recovery of infected vectors	0.0286
q	Transmission rate of asymptomatic infectious class to symptomatic infectious plants class	0.3
φ	Spreading rate of Xcm bacteria from symptomatic infectious plant to the soil	0.89
K	Half saturation constant of Xcm bacteria in the environment	1,000
μ_b	Rate of natural clearance of bacteria in the environment	0.01

The positivity and boundedness of the model solution can be explored by considering the invariant region of the model, derived as follows:

From the system (4), we have

$$ {}^{C}D^{\omega}N_p \le b_p^{\omega} - \alpha_p^{\omega}N_p, \tag{5} $$

$$ N_p(t) \le \frac{b_p^{\omega}}{\alpha_p^{\omega}} + \Big(N_p(0) - \frac{b_p^{\omega}}{\alpha_p^{\omega}}\Big)E_{\omega}(-\alpha_p^{\omega}t^{\omega}). \tag{6} $$

Therefore, the invariant region for N_p is given by

$$ \Lambda_1 = \{S_p(t), A_p(t), I_p(t) \in \mathbb{R}_+^3 : N_p(0) \le N_p(t) \le \frac{b_p^{\omega}}{\alpha_p^{\omega}}, \forall t \ge 0\}. \tag{7} $$

Again, from the system (4), we have

$$ {}^{C}D^{\omega}N_v \le b_v^{\omega} - \mu_v^{\omega}N_v, \tag{8} $$

$$ N_v(t) \le \frac{b_v^{\omega}}{\mu_p^{\omega}} + \Big(N_v(0) - \frac{b_v^{\omega}}{\mu_v^{\omega}}\Big)E_{\omega}(-\mu_v^{\omega}t^{\omega}). \tag{9} $$

Therefore, the invariant region for N_v is given by

$$ \Lambda_2 = \{S_v(t), I_v(t) \in \mathbb{R}_+^2 : N_v(0) \le N_v(t) \le \frac{b_v^{\omega}}{\mu_v^{\omega}}, \forall t \ge 0\}. \tag{10} $$

Furthermore,

$$ \Lambda_3 = \{E_b(t) \in \mathbb{R}_+^1, \forall t \ge 0\}. \tag{11} $$

Considering the aforementioned non-negative initial conditions, the proposed model (2) is positive invariant and solutions remain positive and bounded in the region

$$ \Lambda = \{\Lambda_1 \times \Lambda_2 \times \Lambda_3 : \Lambda \in \mathbb{R}_+^6, \forall t \ge 0\}. \tag{12} $$

The disease-free equilibrium $\mathcal{E}_0$ of the model (2) is defined by

$$ \mathcal{E}_0 = (S_p^0, A_p^0, I_p^0, E_b^0, S_v^0, I_v^0) = \Big(\frac{b_p^{\omega}}{\alpha_p^{\omega}}, 0, 0, 0, \frac{b_v^{\omega}}{\mu_v^{\omega}}, 0\Big). \tag{13} $$

For further numerical simulations, we rewrite the model (2) into a compact form by representing it in terms of an IVP given as follows: Let us consider

$$
\begin{cases}
f_1(t,S_p,\ldots,I_v)=b_p^{\omega}-(1-\xi)\left(a^{\omega}\gamma_1\dfrac{S_pI_v}{N_p}+\beta_a^{\omega}\dfrac{S_pA_p}{N_p}+\beta_s^{\omega}\dfrac{S_pI_p}{N_p}+\gamma_2\dfrac{S_pE_b}{N_p(K+E_b)}\right)-\alpha_p^{\omega}S_p,\\
f_2(t,S_p,\ldots,I_v)=(1-\xi)\left(a^{\omega}\gamma_1\dfrac{S_pI_v}{N_p}+\beta_a^{\omega}\dfrac{S_pA_p}{N_p}+\beta_s^{\omega}\dfrac{S_pI_p}{N_p}+\gamma_2\dfrac{S_pE_b}{N_p(K+E_b)}\right)+(1-\delta)\theta^{\omega}I_p-(\alpha_p^{\omega}+q^{\omega})A_p,\\
f_3(t,S_p,\ldots,I_v)=q^{\omega}A_p-(\alpha_p^{\omega}+d^{\omega}+r^{\omega})I_p,\\
f_4(t,S_p,\ldots,I_v)=\phi^{\omega}I_p-(\mu_b^{\omega}+\psi)E_b,\\
f_5(t,S_p,\ldots,I_v)=b_v^{\omega}+\eta^{\omega}I_v-a^{\omega}\gamma_3\dfrac{S_vI_p}{N_p}-\mu_v^{\omega}S_v,\\
f_6(t,S_p,\ldots,I_v)=a^{\omega}\gamma_3\dfrac{S_vI_p}{N_p}-(\eta^{\omega}+\mu_v^{\omega})I_v.
\end{cases}
\tag{14}
$$

By using (14), we have

$$
{}^{C}D^{\omega}\zeta(t)=\Phi(t,\zeta(t)),\ t\in[0,T],\ 0<\omega\le 1, \zeta(0)=\zeta_0, \tag{15}
$$

where

$$
\zeta(t)=\begin{bmatrix} S_p(t)\\ A_p(t)\\ I_p(t)\\ E_b(t)\\ S_v(t)\\ I_v(t)\end{bmatrix},\quad
\zeta_0(t)=\begin{bmatrix} S_{p_0}(t)\\ A_{p_0}(t)\\ I_{p_0}(t)\\ E_{b_0}(t)\\ S_{v_0}(t)\\ I_{v_0}(t)\end{bmatrix},\quad
\Phi(t,\zeta(t))=\begin{bmatrix} f_1(t,S_p,\ldots,I_v)\\ f_2(t,S_p,\ldots,I_v)\\ f_3(t,S_p,\ldots,I_v)\\ f_4(t,S_p,\ldots,I_v)\\ f_5(t,S_p,\ldots,I_v)\\ f_6(t,S_p,\ldots,I_v)\end{bmatrix}. \tag{16}
$$

3.1. *Solution existence*

Here, we check the existence and uniqueness of the solution with the application of some well-known mathematical results. In this regard, let us consider the above given IVP

$$
{}^{C}D^{\omega}\zeta(t)=\Phi(t,\zeta(t)),\ 0<\omega\le 1, \zeta(0)=\zeta_0. \tag{17}
$$

Consider the Volterra integral equation of the given IVP in equation (17)

$$
\zeta(t)=\zeta_0+\frac{1}{\Gamma(\omega)}\int_0^t (t-x)^{\omega-1}\Phi(\zeta(x),x)\mathrm{d}x.
$$

Using the iterative scheme methodology on the non-linear kernel Φ, we define the expression

$$
\zeta_n(t)=\zeta_0+\frac{1}{\Gamma(\omega)}\int_0^t (t-x)^{\omega-1}\Phi(\zeta_{n-1}(x),x)\mathrm{d}x.
$$

Taking $\zeta_0(t)=\zeta_0$, the difference between two successive terms is defined by

$$
\zeta_n(t)-\zeta_{n-1}(t)=\frac{1}{\Gamma(\omega)}\int_0^t (t-x)^{\omega-1}\left[\Phi(\zeta_{n-1}(x),x)-\Phi(\zeta_{n-2}(x),x)\right]\mathrm{d}x.
$$

Choosing $\zeta_n=\zeta_n(t)-\zeta_{n-1}(t)$, we write

$$\zeta_n(t)=\sum_{j=0}^{n}\zeta_j(t).$$

Therefore, we get

$$\left\|\zeta_n(t)\right\|=\left\|\zeta_n(t)-\zeta_{n-1}(t)\right\|$$

$$\left\|\zeta_n(t)\right\|=\left\|\frac{1}{\Gamma(\omega)}\int_0^t(t-x)^{\omega-1}\left[\Phi(\zeta_{n-1}(x),x)-\Phi(\zeta_{n-2}(x),x)\right]\mathrm{dx}\right\|.$$

Then,

$$\left\|\zeta_n(t)\right\|\le\frac{1}{\Gamma(\omega)}\int_0^t(t-x)^{\omega-1}\left\|\Phi(\zeta_{n-1}(x),x)-\Phi(\zeta_{n-2}(x),x)\right\|\mathrm{dx}.$$

By fixing Φ as a Lipschitzian respect to ζ, we get

$$\left\|\zeta_n(t)\right\|\le\frac{L}{\Gamma(\omega)}\int_0^t(t-x)^{\omega\ 1}\left\|\zeta_{n-1}(x)-\zeta_{n-2}(x)\right\|\mathrm{dx}.$$

Therefore, we get the following expression

$$\left\|\zeta_n(t)\right\|\le\frac{L}{\Gamma(\omega)}\int_0^t(t-x)^{\omega\ 1}\left\|\zeta_{n\ 1}(x)\right\|\mathrm{dx}. \tag{18}$$

Theorem 1. The given IVP in equation (17) has a unique solution under the contraction for Φ.

Proof. From equation (18), we have

$$\left\|\zeta_n(t)\right\|\le\frac{L}{\Gamma(\omega)}\int_0^t(t-x)^{\omega-1}\left\|\zeta_{n-1}(x)\right\|\mathrm{dx}.$$

Putting the value of $\|\zeta_{n-1}(t)\|$, we have

$$\left\|\zeta_n(t)\right\|\le\left(\frac{Lt^{\omega}}{\Gamma(\omega+1)}\right)^2\left\|\zeta_{n-2}(t)\right\|.$$

Similarly, for $\|\zeta_{n-2}(t)\|$

$$\left\|\zeta_n(t)\right\|\le\left(\frac{Lt^{\omega}}{\Gamma(\omega+1)}\right)^3\left\|\zeta_{n-3}(t)\right\|.$$

Then, the successive iterations give

$$\left\|\zeta_n(t)\right\|\le\left(\frac{Lt^{\omega}}{\Gamma(\omega+1)}\right)^n\left\|\zeta_0(t)\right\|\le\left(\frac{t^{\omega}}{\Gamma(\omega+1)}\right)^n L^n\max_{t\in[0,T]}\left\|\zeta_0\right\|.$$

If $\zeta(t)=\sum_{j=0}^{n}\zeta_j(t)$, then solution $\zeta(t)$ exists and continuous.

Consider $\zeta(t)=\zeta_n(t)+\Lambda_n(t)$, where $\Lambda_n(t)$ is the amount of error with $\Lambda_n(t)\to 0$ when $n\to\infty$. Then, Now,

$$\zeta(t)-\zeta_0-\frac{1}{\Gamma(\omega)}\int_0^t(t-x)^{\omega-1}\Phi(\zeta(x),x)\mathrm{dx}=\Lambda_n(t)+\frac{1}{\Gamma(\omega)}\int_0^t(t-x)^{\omega-1}\left[\Phi(\zeta(x)-\Lambda_n(x),x)-\Phi(\zeta(x),x)\right]\mathrm{dx}.$$

Applying the norm, we get

$$\left\|\zeta(t)-\zeta_0-\frac{1}{\Gamma(\omega)}\int_0^t(t-x)^{\omega-1}\Phi(\zeta(x),x)\mathrm{dx}\right\|\le\|\Lambda_n(t)\|+\frac{1}{\Gamma(\omega)}\int_0^t(t-x)^{\omega-1}\times\|\Phi(\zeta(x)-\Lambda_n(x),x)-\Phi(\zeta(x),x)\|\mathrm{dx}$$

$$\|\Lambda_n(t)\|+\frac{Lt^{\omega}}{\Gamma(\omega+1)}\|\Lambda_{n-1}(t)\|. \tag{19}$$

If $n\to\infty$, the right-hand side of equation (19) converges to zero.

Then,

$$\zeta(t)=\zeta_0+\frac{1}{\Gamma(\omega)}\int_0^t(t-x)^{\omega-1}\Phi(\zeta(x),x)\mathrm{dx},$$

which gives the existence of the solution $\zeta(t)$.

Now, for the uniqueness, consider two different solutions $\zeta(t)$ and $\zeta_1(t)$. Then,

$$\begin{aligned}\|\zeta(t)-\zeta_1(t)\|&\le\frac{Lt^{\omega}}{\Gamma(\omega+1)}\|\zeta(t)-\zeta_1(t)\|\\&\le\left(\frac{Lt^{\omega}}{\Gamma(\omega+1)}\right)^2\|\zeta(t)-\zeta_1(t)\|\\&\quad\vdots\\&\le\left(\frac{Lt^{\omega}}{\Gamma(\omega+1)}\right)^n\|\zeta(t)-\zeta_1(t)\|\end{aligned}$$

when $n\to\infty$, $L^{\infty}\to 0$, which gives $\zeta(t)$ and $\zeta_1(t)$.

Hence, there exists a unique solution for the proposed IVP (17). Therefore, we conclude that the proposed fractional-order model (2) has a unique solution.

3.2. *Solution stability*

Theorem 2. [48] Consider a completely generalized metric space $(\mathcal{Z},R)$. Assume $A:\mathcal{Z}\to\mathcal{Z}$ is a strictly contractive operator. If there exists an integer $v\ge 0$ with $R(A^{v+1}d, A^{v}d)<\infty$ for some $d\in\mathcal{Z}$, then

(a) $\lim_{l\to+\infty}A^{l}d=d^{*}$ is the unique fixed point of A in

$$\mathcal{Z}^{*}:=\left\{d_1\in\mathcal{Z}:R(A^{v}d,d_1)<\infty\right\}. \tag{20}$$

(b) If $d_1\in\mathcal{Z}^{*}$, then $R(d_1,d^{*})\le(1/(1-K))R(Ad_1,d_1)$. In our case, $\mathcal{Z}:=C(I,\mathbb{R})$ and $I:=[0,T]$.

Theorem 3. Consider $\Phi:I\times\mathbb{R}\to\mathbb{R}$ is continuous and satisfying

$$|\Phi(t,\zeta^{*})-\Phi(t,\zeta^{**})|\le L_p|\zeta^{*}-\zeta^{**}|, \tag{21}$$

$\forall t\in I,\zeta^{*},\zeta^{**}\in\mathbb{R}$, and for some $L_p>0$. If $\zeta:I\to\mathbb{R}$ is absolutely continuous and satisfies

$$\left|{}^{C}D^{\omega}\zeta(t)-\Phi(t,\zeta(t))\right|\leq\epsilon(t), \tag{22}$$

$\forall t\in I$, where $\epsilon>0$ and $\rho(t)$ is a positive, non-decreasing, and continuous function. Then, there exists a solution ζ^{*} of equation (17), such that

$$\left|\zeta(t)-\zeta^{*}(t)\right|\leq\left(\frac{L_p+\delta}{\delta}\right)\frac{M\mathbb{E}_{\omega}\left((L_p+\delta)T^{\omega}\right)}{\Gamma(\omega+1)},\epsilon\rho(t), \tag{23}$$

where

$$M=\sup_{s\in[0,T]}\left(\frac{(s)^{\omega}}{\mathbb{E}_{\gamma}\left((L_p+\delta)(s)^{\omega}\right)}\right) \tag{24}$$

and δ is a positive constant.

Proof. We define the metric d on space $\mathcal{Z}$ by

$$d(\zeta^{*},\zeta^{**})=\inf\left\{D\in[0,\infty]:\frac{|\zeta^{*}(t)-\zeta^{**}(t)|}{\mathbb{E}_{\gamma}\left((L_p+\delta)(t)^{\omega}\right)}\leq D\rho(t),\forall t\in I\right\}. \tag{25}$$

Define an operator $\mathcal{A}:\mathcal{Z}\to\mathcal{Z}$, such that

$$(\mathcal{A}\zeta)(t):=\zeta(0)+\frac{1}{\Gamma(\omega)}\int_0^t(t-s)^{\omega-1}\Phi(s,\zeta(s))\mathrm{d}s. \tag{26}$$

It is easy to say $d(\mathcal{A}\zeta_0,\zeta_0)<\infty$ and $\{\zeta\in\mathcal{Z}:d(\zeta_0,\zeta)<\infty\}=X,\forall\zeta_0\in\mathcal{Z}$.

The operator $\mathcal{A}$ is a strictly contractive operator, which can be seen by the following expression:

$$\begin{aligned}
|(\mathcal{A}\zeta^{*})(t)-(\mathcal{A}\zeta^{**})(t)|&\leq\left|\int_0^t\frac{(t-\xi)^{\omega-1}}{\Gamma(\omega)}\{\Phi(\xi,\zeta^{*}(\xi))-\Phi(\xi,\zeta^{**}(\xi))\}\mathrm{d}\xi\right|\\
&\leq\frac{1}{\Gamma(\omega)}\int_0^t(t-\xi)^{\omega-1}|\Phi(\xi,\zeta^{*}(\xi))-\Phi(\xi,\zeta^{**}(\xi))|\mathrm{d}\xi\\
&\leq L_p\int_0^t(t-\xi)^{\omega-1}\frac{|\zeta^{*}(\xi)-\zeta^{**}(\xi)|}{\Gamma(\omega)}\mathrm{d}\xi\\
&\leq\frac{L_p}{\Gamma(\omega)}\int_0^t(t-\xi)^{\omega-1}\frac{|\zeta^{*}(\xi)-\zeta^{**}(\xi)|}{\mathbb{E}_{\omega}\left((L_p+\delta)(\xi)^{\omega}\right)}\mathbb{E}_{\omega}\left((L_p+\delta)(\xi)^{\omega}\right)\mathrm{d}\xi\\
&\leq\frac{L_pd(\zeta^{*},\zeta^{**})}{\Gamma(\omega)}\int_0^t(t-\xi)^{\omega-1}\rho(\xi)\mathbb{E}_{\omega}\left((L_p+\delta)(\xi)^{\omega}\right)\mathrm{d}\xi,\ \text{for all } t\in I
\end{aligned} \tag{27}$$

Since ρ is non-decreasing, we have

$$|(\mathcal{A}\zeta^*)(t)-(\mathcal{A}\zeta^{**})(t)| \leq \frac{L_p d(\zeta^*,\zeta^{**})}{\Gamma(\omega)}\rho(t)\int_0^t (t-\xi)^{\omega-1}\mathbb{E}_\omega\left((L_p+\delta)(\xi)^\omega\right)\mathrm{d}\xi$$

$$\leq \frac{L_p d(\zeta^*,\zeta^{**})}{L_p+\delta}\left(\mathbb{E}_\omega\left((L_p+\delta)(\xi)^\omega\right)-1\right)\rho(t)$$

$$\leq \frac{L_p d(\zeta^*,\zeta^{**})}{L_p+\delta}\left(\mathbb{E}_\omega\left((L_p+\delta)(\xi)^\omega\right)\right)\rho(t), \text{ for all } t\in I. \tag{28}$$

Therefore,

$$d(\mathcal{A}\zeta^*,\mathcal{A}\zeta^{**}) \leq \frac{L_p}{L_p+\delta}d(\zeta^*,\zeta^{**}),$$

which gives that the operator $\mathcal{A}$ is a strictly contractive operator. Now, since we have

$$\left|{}^C D^\omega \zeta(t)-\Phi(t,\zeta(t))\right| \leq \epsilon\rho(t), \tag{29}$$

then

$$\left|\zeta(t)-\mathcal{A}\zeta(t),\zeta(t))\right| \leq \frac{\epsilon}{\Gamma(\omega)}\rho(t)\int_0^t (t-\xi)^{\omega-1}\rho(\xi)\mathrm{d}\xi, \tag{30}$$

which implies that

$$\frac{\left|\zeta(t)-\mathcal{A}\zeta(t),\zeta(t))\right|}{\mathbb{E}_\omega\left((L_p+\delta)(\xi)^\omega\right)} \leq \frac{\epsilon}{\Gamma(\omega+1)}\rho(t)\frac{(t-\xi)^\omega}{\mathbb{E}_\omega\left((L_p+\delta)(\xi)^\omega\right)}$$

$$\leq \frac{\epsilon M}{\Gamma(\omega+1)}\rho(t). \tag{31}$$

Therefore,

$$d(\zeta,\mathcal{A}\zeta) \leq \epsilon\frac{M}{\Gamma(\omega+1)}.$$

By using Theorem 2, there is a solution ζ^* of IVP (17), such that

$$d(\zeta,\zeta^*) \leq \epsilon\left(\frac{L_p+\delta}{\delta}\right)\frac{M}{\Gamma(\omega+1)}.$$

So that,

$$|\zeta(t)-\zeta^*(t)| \leq \left(\frac{L_p+\delta}{\delta}\right)\frac{M\mathbb{E}_\omega\left((L_p+\delta)T^\omega\right)}{\Gamma(\omega+1)},\epsilon\rho(t) \text{ for all } t\in[0,T].$$

Hence, the solution of the proposed model is stable.

4. Numerical analysis on the model

In this section, we perform the necessary numerical simulations (solution derivation, error estimation, and stability) to derive the solution of the proposed fractional-order model (2) by using the L1-PC scheme [41].

Consider the above given IVP for $0 < \omega < 1$,

$$^{C}D^{\omega}\zeta(t) = \Phi(t, \zeta(t)), t \in [0, T], \ \zeta(0) = \zeta_0. \tag{32}$$

where $^{C}D^{\omega}$ represents the Caputo derivatives and $\Phi : [0, T] \times D \to \mathbb{R}, D \subset \mathbb{R}$. Split the time span [0, T] into N subintervals. Take a uniform grid with step size of $h = \frac{T}{N}$ with $t_k = kh, k = 0, 1, \cdots N$.

4.1. *Derivation of the solution*

According to the L1-PC method, the Caputo fractional derivative is numerically defined by

$$\begin{aligned}
\left[{}^{C}D^{\omega}\zeta(t) \right]_{t=t_n} &= \frac{1}{\Gamma(1-\omega)} \int_0^{t_k} (t_n - s)^{-\omega} \zeta'(s) \mathrm{d}s \\
&= \frac{1}{\Gamma(1-\omega)} \sum_{k=0}^{n-1} \int_{t_k}^{t_{k+1}} (t_n - s)^{-\omega} \zeta'(s) \mathrm{d}s \\
&\approx \frac{1}{\Gamma(1-\omega)} \sum_{k=0}^{n-1} \int_{t_k}^{t_{k+1}} (t_n - s)^{-\omega} \frac{\zeta(t_{k+1}) - \zeta(t_k)}{h} \mathrm{d}s \\
&= \sum_{k=0}^{n-1} b_{n-k-1} (\zeta(t_{k+1}) - \zeta(t_k)),
\end{aligned} \tag{33}$$

where

$$b_k = \frac{h^{-\omega}}{\Gamma(2-\omega)} \left[(k+1)^{1-\omega} - k^{1-\omega} \right].$$

We approximate $^{C}D^{\omega}\zeta(t)$ by the formula (33), and put it into (32) to get

$$\left[{}^{C}D^{\omega}\zeta(t) \right]_{t=t_n} = \sum_{k=0}^{n-1} b_{n-k-1} (\zeta(t_{k+1}) - \zeta(t_k)) = \Phi(t_n, \zeta_n), \tag{34}$$

where ζ_k defines the approximate value of the solution of (32) at $t = t_k$ and

$$b_{n-k-1} = \frac{h^{-\omega}}{\Gamma(2-\omega)} \left[(n-k)^{1-\omega} - (n-k-)^{1-\omega} \right].$$

(34) can be rewritten as:

$$b_{n-1}(\zeta_1 - \zeta_0) + b_{n-2}(\zeta_2 - \zeta_1) + \cdots + b_0(\zeta_n - \zeta_{n-1}) = \Phi(t_n, \zeta_n). \tag{35}$$

After rewriting the terms (35), we get the following from

$$b_0\zeta_n = b_0\zeta_{n-1} - \sum_{k=0}^{n-2} b_{k+1}\zeta_{n-1-k} + \sum_{k=1}^{n-1} b_k\zeta_{n-1-k} + \Phi(t_n,\zeta_n). \tag{36}$$

Substituting

$$b_0 = \frac{h^{-\omega}}{\Gamma(2-\omega)} \text{ and } b_k = \frac{h^{-\omega}}{\Gamma(2-\omega)}\left[(n-k)^{1-\omega} - (n-k-)^{1-\omega}\right]$$

in (35), we get

$$\begin{aligned}\zeta_n &= \zeta_{n-1} - (2^{1-\omega} - 1^{1-\omega})\zeta_{n-1} - \sum_{k=1}^{n-2}((2+k)^{1-\omega} - (1+k)^{(1-\omega)})\zeta_{n-1-k} + \sum_{k=1}^{n-2}((1+k)^{1-\omega} - (k)^{(1-\omega)})\zeta_{n-1-k} \\ &\quad +(n^{1-\omega} - (n-1)^{1-\omega})\zeta_0 + \Gamma(2-\omega)h^{\omega}\Phi(t_n,\zeta_n) \\ &= (n^{1-\omega} - (n-1)^{1-\omega})\zeta_0 + \sum_{k=1}^{n-1}[2(n-k)^{1-\omega} - (n+1-k)^{(1-\omega)} - (n-1-k)^{(1-\omega)}]\zeta_k \\ &\quad +\Gamma(2-\omega)h^{\omega}\Phi(t_n,\zeta_n)\end{aligned} \tag{37}$$

Define

$$a_k := (k+1)^{1-\omega} - k^{1-\omega}. \tag{38}$$

Remark that $a_k's$ has the following characteristics:

- $a_k > 0, k = 0,1,\cdots n-1.$
- $a_0 = 1 > a_1 > \cdots > a_k$ and $a_k \to 0$ as $k \to \infty.$
- $\sum_{k=0}^{n-1}(a_k - a_{k+1}) + a_n = (1-a_1) + \sum_{k=1}^{n-2}(a_k - a_{k+1}) + a_{n-1} = 1.$

In view of equations (38) and (37), take the following form:

$$\zeta_n = a_{n-1}\zeta_0 + \sum_{k=1}^{n-1}(a_{n-1-k} - a_{n-k})\zeta_k + \Gamma(2-\omega)h^{\omega}\Phi(t_n,\zeta_n). \tag{39}$$

We can see that equation (39) is of the form $\zeta_n = g + N(\zeta_n),$ if we identify

$$g = a_{n-1}\zeta_0 + \sum_{k=1}^{n\ 1}(a_{n-1-k} - a_{n-k})\zeta_k$$

and

$$N(\zeta_n) = \Gamma(2-\omega)h^{\omega}\Phi(t_n,\zeta_n).$$

Hence, using the scheme of Daffatardar-Gejji-Jafari method gives an approximate value of ζ_n given by

$$\zeta_{n,0} = g = a_{n-1}\zeta_0 + \sum_{k=1}^{n-1}(a_{n-1-k} - a_{n-k})\zeta_k,$$

$$\zeta_{n,0} = N(\zeta_{n,0}) = \Gamma(2-\omega)h^{\omega}\Phi(t_n, \zeta_n),$$

$$\zeta_{n,2} = N(\zeta_{n,0} + \zeta_{n,1} - N(\zeta_{n,0}).$$

The three-term approximation of $\zeta_n \approx \zeta_{n,0} + \zeta_{n,0} + \zeta_{n,2}$. Therefore, this approximated solution of the DGJ scheme gives the following predictor-corrector algorithm called the L1-PC method.

$$\begin{aligned}
\zeta_n^p &= a_{n-1}\zeta_0 + \sum_{k=1}^{n-1}(a_{n-1-k} - a_{n-k})\zeta_k,\\
z_n^p &= N(\zeta_n) = \Gamma(2-\omega)h^{\omega}\Phi(t_n, \zeta_n^p),\\
\zeta_n^c &= \zeta_n^p + \Gamma(2-\omega)h^{\omega}\Phi(t_n, \zeta_n^p + z_n^p),
\end{aligned} \tag{40}$$

where ζ_n^p and z_n^p are the predictors and ζ_n^c is the corrector.

Using the above given methodology, the approximation equations of the proposed model (2) in terms of L1-PC method are derived as follows:

$$\begin{cases}
S_{pn}^{\ c} = S_{pn}^{\ p} + \Gamma(2-\omega)h^{\omega} f_1(t_n, S_{pn}^{\ p} + z_{1n}^p, \ldots, I_{vn}^{\ p} + z_{6n}^p),\\
A_{pn}^{\ c} = A_{pn}^{\ p} + \Gamma(2-\omega)h^{\omega} f_2(t_n, S_{pn}^{\ p} + z_{1n}^p, \ldots, I_{vn}^{\ p} + z_{6n}^p),\\
I_{pn}^{\ c} = I_{pn}^{\ p} + \Gamma(2-\omega)h^{\omega} f_3(t_n, S_{pn}^{\ p} + z_{1n}^p, \ldots, I_{vn}^{\ p} + z_{6n}^p),\\
E_{bn}^{\ c} = E_{bn}^{\ p} + \Gamma(2-\omega)h^{\omega} f_4(t_n, S_{pn}^{\ p} + z_{1n}^p, \ldots, I_{vn}^{\ p} + z_{6n}^p),\\
S_{vn}^{\ c} = S_{vn}^{\ p} + \Gamma(2-\omega)h^{\omega} f_5(t_n, S_{pn}^{\ p} + z_{1n}^p, \ldots, I_{vn}^{\ p} + z_{6n}^p),\\
I_{vn}^{\ c} = I_{vn}^{\ p} + \Gamma(2-\omega)h^{\omega} f_6(t_n, S_{pn}^{\ p} + z_{1n}^p, \ldots, I_{vn}^{\ p} + z_{6n}^p),
\end{cases} \tag{41}$$

where

$$\begin{cases}
S_{pn}^{\ p} = a_{n-1}S_{p_0} + \sum_{k=1}^{n-1}(a_{n-1-k} - a_{n-k})S_{p_k},\\
A_{pn}^{\ p} = a_{n-1}A_{p_0} + \sum_{k=1}^{n-1}(a_{n-1-k} - a_{n-k})A_{p_k},\\
I_{pn}^{\ p} = a_{n-1}I_{p_0} + \sum_{k=1}^{n-1}(a_{n-1-k} - a_{n-k})I_{p_k},\\
E_{bn}^{\ p} = a_{n-1}E_{b_0} + \sum_{k=1}^{n-1}(a_{n-1-k} - a_{n-k})E_{b_k},\\
S_{vn}^{\ p} = a_{n-1}S_{v_0} + \sum_{k=1}^{n-1}(a_{n-1-k} - a_{n-k})S_{v_k},\\
I_{vn}^{\ p} = a_{n-1}I_{v_0} + \sum_{k=1}^{n-1}(a_{n-1-k} - a_{n-k})I_{v_k},
\end{cases} \tag{42}$$

and

$$\begin{cases} z_{1n}^p = N(S_{p_n}) = \Gamma(2-\omega)h^{\omega}\mathrm{f}_1(t_n, S_{pn}^{\ p}, \ldots, I_{vn}^{\ p}), \\ z_{2n}^p = N(A_{p_n}) = \Gamma(2-\omega)h^{\omega}\mathrm{f}_2(t_n, S_{pn}^{\ p}, \ldots, I_{vn}^{\ p}), \\ z_{3n}^p = N(I_{p_n}) = \Gamma(2-\omega)h^{\omega}\mathrm{f}_3(t_n, S_{pn}^{\ p}, \ldots, I_{vn}^{\ p}), \\ z_{4n}^p = N(E_{b_n}) = \Gamma(2-\omega)h^{\omega}\mathrm{f}_4(t_n, S_{pn}^{\ p}, \ldots, I_{vn}^{\ p}), \\ z_{5n}^p = N(S_{v_n}) = \Gamma(2-\omega)h^{\omega}\mathrm{f}_5(t_n, S_{pn}^{\ p}, \ldots, I_{vn}^{\ p}), \\ z_{6n}^p = N(I_{v_n}) = \Gamma(2-\omega)h^{\omega}\mathrm{f}_6(t_n, S_{pn}^{\ p}, \ldots, I_{vn}^{\ p}). \end{cases} \tag{43}$$

4.2 *Error analysis*

The brief analysis on the error estimation of L1-PC scheme has been given in the studies [41, 49, 50] and now investigated below. The error estimate is given by

$$\left| [{}^C D^{\omega}\zeta(t)]_{t=t_n} - \sum_{k=0}^{n-1} b_{n-k-1}(\zeta_{k+1} - \zeta_k) \right| \leq Ch^{2-\omega}, \tag{44}$$

here C is a positive constant depends on ω and ζ.

Derive r_n by

$$r_n := \Gamma(2-\omega)h^{\omega}\Big[[{}^C D^{\omega}\zeta(t)]_{t=t_n} - \sum_{k=0}^{n-1} b_{n-k-1}(\zeta_{k+1} - \zeta_k)\,||\Big]. \tag{45}$$

In view of (44),

$$|\, r_n | = \Gamma(2-\omega)h^{\omega}\left| [{}^C D^{\omega}\zeta(t)]_{t=t_n} - \sum_{k=0}^{n-1} b_{n-k-1}(\zeta_{k+1} - \zeta_k)\,|| \right| \leq \Gamma(2-\omega)Ch^2. \tag{46}$$

To derive the error estimation, we will use the lemmas given below.

Lemma 1. [51] For $0 < \omega < 1$ and $a_k's$ (as given in equation (38)), we have

$$k^{-\omega}a_{k-1}^{-1} \leq \frac{1}{1-\omega}, k = 1, 2, \cdots, N.$$

Lemma 2. [41] Consider $\zeta(t_k)$ as exact solution of the proposed IVP and ζ_k^p be the approximate solution calculated from the algorithm (40). Then, for $0 < \omega < 1$, we have

$$|\, \zeta(t_k) - \zeta_k^p \,| \leq Ca_{k-1}^{-1}, k = 1, 2, \cdots N,$$

where $a'_k\, s$ are given in equation (38).

Lemma 3. [41] Consider $\zeta(t_k)$ as exact solution of the proposed IVP and ζ_k^p be the approximate value evaluated from equation (40). Then, for $0 < \omega < 1$, we have

$$|\, \zeta(t_k) - \zeta_k^p \,| \leq C_{\omega}T^{\omega}h^{\ -\omega}, k = 1, 2, \cdots N,$$

where $C_{\omega} = C/(1-\omega)$.

Theorem 4. Consider $\zeta(t)$ as exact solution of the proposed IVP (32), $\Phi(t, \zeta(t))$ satisfies the Lipschitz property respect to the variable ζ with a constant L, and $\Phi(t, \zeta(t)), \zeta(t) \in C^1[0, T]$. Also, ζ_k^c defines the approximate solutions at $t = t_k$ calculated by using L1-PC method. Then, for $0 < \omega < 1$, we have

$$|\zeta(t_k)-\zeta_k^c| \le C_1 T^{\omega} h^{2-\omega}, k=1,2,\cdots N, \tag{47}$$

where $C_1 = d/(1-\omega)$ and d is a constant.

Proof. Let $e_k = \zeta(t_k)-\zeta_k^c$ and $e_k^p = \zeta(t_k)-\zeta_k^p$. Using equations (32), (40), and (45), we get

$$e_n = e_n^p + \Gamma(2-\omega)h^{\omega}(\Phi(t_n,\zeta(t_n))+N(\zeta(t_n)))-\Phi(t_n,\zeta_n^p+N((\zeta_n^p))).$$

Further, observe that

$$\begin{aligned}
|e_n| &\le |e_n^p| + \Gamma(2-\omega)h^{\omega}|\Phi(t_n,\zeta(t_n))+N(\zeta(t_n)))-\Phi(t_n,\zeta_n^p+N((\zeta_n^p)))| \\
&\le |e_n^p| + L\Gamma(2-\omega)h^{\omega}|\zeta(t_n)-\zeta_n^p+N(\zeta(t_n)))-N((\zeta_n^p))| \\
&\le |e_n^p| + L\Gamma(2-\omega)h^{\omega}|e_n^p| + L^2(\Gamma(2-\omega))^2 h^{2\omega}|\zeta(t_n)-\zeta_n^p| \\
&\le |e_n^p| + L\Gamma(2-\omega)h^{\omega}|e_n^p| + L^2(\Gamma(2-\omega))^2 h^{2\omega}|e_n^p| \\
&\le [1+L\Gamma(2-\omega)h^{\omega}+L^2(\Gamma(2-\omega))^2 h^{2\omega}]|e_n^p|.
\end{aligned} \tag{48}$$

Using Lemma 3 in equation (48), we get

$$\begin{aligned}
|e_n| &\le [1+L\Gamma(2-\omega)h^{\omega}+L^2(\Gamma(2-\omega))^2 h^{2\omega}]C_{\omega}T^{\omega}h^{2-\omega} \\
&\le [1+L\Gamma(2-\omega)+L^2(\Gamma(2-\omega))^2]C_{\omega}T^{\omega}h^{2-\omega}.
\end{aligned}$$

Therefore,

$$|e_n| \le C_1 T^{\omega} h^{2-\omega},$$

where C_1 is a constant defined above.

4.3. *Stability analysis*

Consider [41] that ζ_n^c and $v_n^c (n=1,2\cdots,N)$ are two solutions calculated by the numerical scheme (40). For $\delta_0 = |\zeta_0 - v_0|$, there exists two positive quantities k and h' such that

$$|\zeta_n^c - v_n^c| \le k\delta_0, \ \text{for } h\in(0,h'), \ 1\le n\le N,$$

Here, h is the step size given in equation (32).

Theorem 5. Suppose $\Phi(t,\zeta)$ follows the Lipschitz property with respect to the variable ζ with a constant L and ζ_n^c $(n=1,2,\cdots,N)$ are the solutions established from the scheme (40), then the scheme (40) is stable.

Proof. We have to prove that

$$|\zeta_n^c - v_n^c| \le C|\zeta_0 - v_0|.$$

Denote by $\eta_0 := (1+(L\Gamma(2-\omega))+L^2(\Gamma(2-\omega))^2 h^{\omega})$. Note that

$$|\zeta_n^c - v_n^c| \le |\zeta_n^p - v_n^p| + L\Gamma(2-\omega)h^{\omega}(|\zeta_n^p - v_n^p| + |N(\zeta_n^p)-N(v_n^p)|). \tag{49}$$

Further, observe that

$$
\begin{aligned}
|\zeta_n^c - v_n^c| &= |a_{n-1}(\zeta_0 - v_0) + \sum_{k=1}^{n-1}(a_{n-1-k} - a_{n-k})(\zeta_k - v_k)| \\
&\leq a_{n-1}|\zeta_0 - v_0| + \sum_{k=1}^{n-1}(a_{n-1-k} - a_{n-k})|\zeta_k - v_k| \\
&\leq |\zeta_0 - v_0| + \sum_{k=1}^{n-1}(a_{n-1-k} - a_{n-k})|\zeta_k - v_k|.
\end{aligned}
$$

Using discrete form of Gronwall's inequality and equation (38), we obtain

$$
|\zeta_n^p - v_n^p| \leq c|\zeta_0 - v_0 \tag{50}
$$

where c is a constant and

$$
\begin{aligned}
|N(\zeta_n^p) - N(v_n^p)| &= |\Gamma(2-\omega)h^{\omega}(\Phi(t_n,\zeta_n^p)) - \Phi(t_n, v_n^p))| \\
&\leq L\Gamma(2-\omega)h^{\omega}|\zeta_n^p - v_n^p|.
\end{aligned} \tag{51}
$$

Using (50) and (51) in (49), we get

$$
\begin{aligned}
|\zeta_n^c - v_n^c| &\leq |\zeta_n^p - v_n^p| + L\Gamma(2-\omega)h^{\omega}|\zeta_n^p - v_n^p| + L^2(\Gamma(2-\omega))^2 h^{2\omega}|\zeta_n^p - v_n^p| \\
&\leq |\zeta_n^p - v_n^p| + L\Gamma(2-\omega)h^{\omega}|\zeta_n^p - v_n^p| + L^2(\Gamma(2-\omega))^2 h^{\omega}|\zeta_n^p - v_n^p| \\
&\leq (1 + L\Gamma(2-\omega) + L^2(\Gamma(2-\omega))^2)h^{\omega}|\zeta_n^p - v_n^p| \\
&\leq \eta_0 c|\zeta_0 - v_0| \leq C|\zeta_0 - v_0|,
\end{aligned}
$$

where C is a constant.

5. Graphical simulations

In this section, we perform the graphical simulations to understand the behavior of the proposed model in a time range $t \in [0,20]$. The initial conditions are used as follows: $S_p(0) = 4{,}000$, $A_p(0) = 500$, $I_p(0) = 200$, $E_b(0) = 500$, $S_v(0) = 3{,}500$, and $I_v(0) = 500$. The parameter values are taken from Table 1 along with the control measures; the participatory community education programs ($\xi = 0.7$), vertical transmission control ($\delta = 0.6$), and the clearance of Xcm bacteria in the soil ($\psi = 0.5$).

In Figure 2, the variations in the susceptible plants S_p and susceptible vectors S_v are plotted at fractional-order values $\omega = 0.9$ and $\omega = 0.8$, along with the integer-order case $\omega = 1$. Here, we notice that as the fractional order decreases, the susceptible plant and vector population also decreases.

In Figure 3, the changes in the population of asymptomatic infected plants A_p and infected plants Ip are plotted at the same orders: $\omega = 1,0.9$ and $\omega = 0.8$. Here, we notice the variations at given fractional orders after the time range [0, 5]. Between the time range [5, 20] months, when the fractional order decreases, the infection slightly increases.

In Figure 4, the variations in the Xcm bacteria in the soil E_b and infected vectors I_v are plotted at the given fractional-order values. From Figure 4(b), we notice that, reaching the end point of the time $t = 20$, all fractional-order outputs nearly converge.

In Figure 5, we plotted the infectious class I_p versus S_p (5(a)), the infectious class I_p versus S_v (5(b)), and the infectious class I_p versus I_v (5(c)).

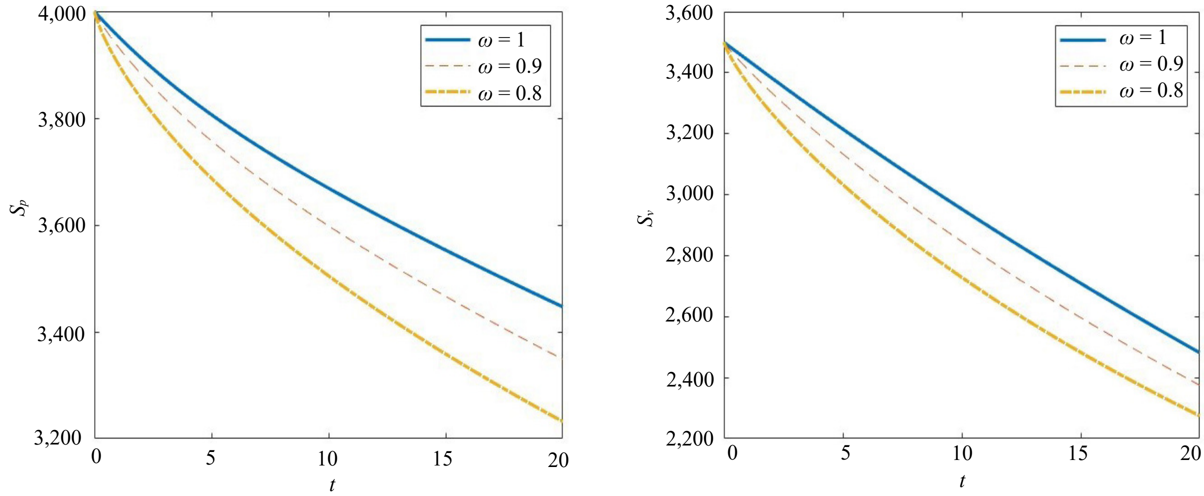

(a) Susceptible plants S_p (b) Susceptible vectors S_v

Figure 2. Variations in the susceptible population S_p and S_v at fractional order values ω

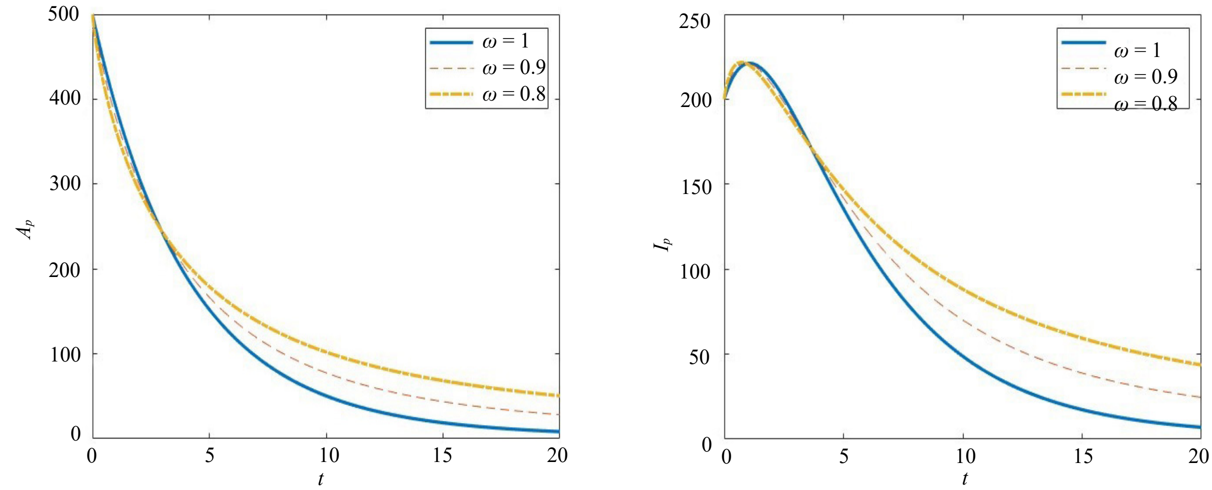

(a) Asymptomatic infected plants A_p (b) Infected plants I_p

Figure 3. Variations in the A_p and I_p population at fractional order values ω

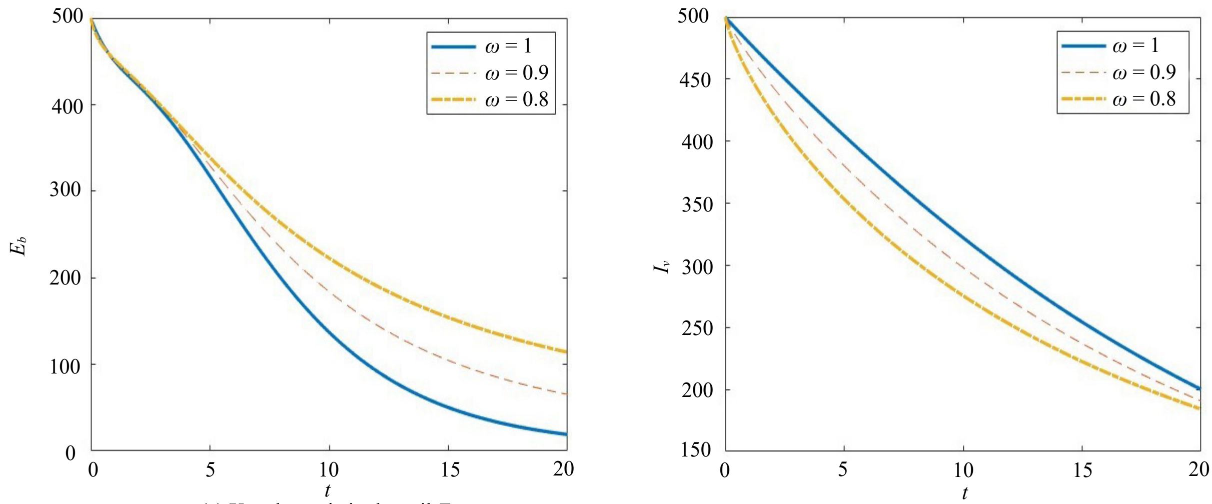

(a) Xcm bacteria in the soil E_b (b) Infected vectors I_v

Figure 4. Variations in the E_b and I_v population at fractional order values ω

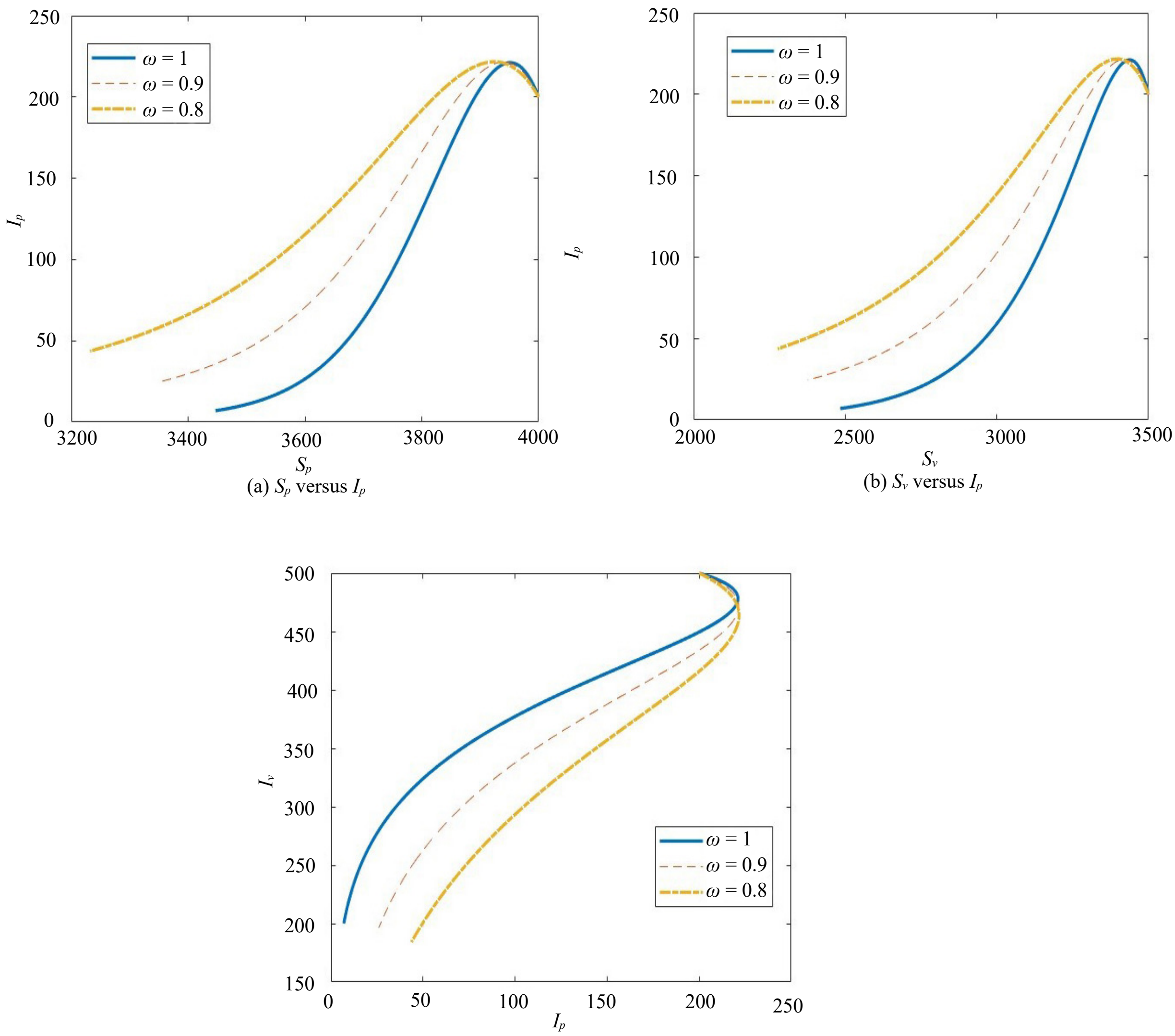

(c) I_p versus I_v

Figure 5. Variations in the infected plant population I_p versus S_p, S_v, and I_v classes at fractional order values ω

From the given graphical simulations, we notice that the fractional-order values result in variations in the behavior of the model dynamics. Such effects cannot be captured by using integer-order derivatives, which justifies the advantage of fractional derivatives. The graphs are plotted using MATLAB-2021a.

6. Conclusion

A fractional-order mathematical model of the BXW disease using Caputo derivatives has been considered in this study. The proposed model has been numerically solved using an L1-based predictor-corrector scheme. The analysis of the stability and error approximation of the proposed method has been established to justify the efficiency of the scheme. The graphical simulations justified the fact that fractional-order values result in variations in the model dynamics and that variations cannot be captured in the case of the integer-order model. In the future, some other fractional-order operators can be incorporated to analyze the proposed model's dynamics. Moreover, some other fractional-order models can be proposed to forecast the outbreaks of BXW.

Data availability

The data used in this research is available/mentioned in the manuscript.

Conflict of interest

This work does not have any conflicts of interest.

References

[1] Ssekiwoko F, Taligoola, HK, Tushemereirwe WK. *Xanthomonas campestris* pv *musacearum* host range in Uganda. *African Crop Science Journal*. 2006; 14(2): 111-120. Available from: https://doi.org/10.4314/acsj.v14i2.27917.

[2] Buregyeya H, Kubiriba J, Tusiime G, Kityo R, Ssekiwoko F, Tushemerierwe WK. Role of birds & bats in long distance transmission of banana bacterial wilt in Uganda. *International Journal of Agriculture Innovations and Research*. 2014; 2(4): 636-640.

[3] Kubiriba J, Tushemereirwe WK. Approaches for the control of Banana Xanthomonas Wilt in East and Central Africa. *African Journal of Plant Science*. 2014; 8(8): 398-404.

[4] Nakato V, Mahuku G, Coutinho T. *Xanthomonas campestris* pv. *musacearum*: A major constraint to banana, plantain and enset production in central and east Africa over the past decade. *Molecular Plant Pathology*. 2018; 19(3): 525-536. Available from: https://doi.org/10.1111/mpp.12578.

[5] Kubiriba J, Karamura EB, Jogo W, Tushemereirwe WK, Tinzaara W. Community mobilization: A key to effective control of Banana Xanthomonas Wilt. *Journal of Development and Agricultural Economics*. 2012; 4(5): 125-131.

[6] Ocimati W, Nakato GV, Fiaboe KM, Beed F, Blomme G. Incomplete systemic movement of *Xanthomonas campestris* pv. *musacearum* and the occurrence of latent infections in Xanthomonas wilt-infected banana mats. *Plant Pathology*. 2015; 64(1): 81-90. Available from: https://doi.org/10.1111/ppa.12233.

[7] Ntamwira J, Blomme G, Bahati L, Ocimati W. Effect of timing of diseased plant cutting, altitude and banana cultivar on efficacy of singly removing Xanthomonas wilt infected banana plants. *European Journal of Plant Pathology*. 2019; 154(2): 477-489. Available from: https://doi.org/10.1007/s10658-019-01671-9.

[8] Uwamahoro F, Berlin A, Bylund H, Bucagu C, Yuen J. Management strategies for Banana Xanthomonas Wilt in Rwanda include mixing indigenous and improved cultivars. *Agronomy for Sustainable Development*. 2019; 39: 22. Available from: https://doi.org/10.1007/s13593-019-0569-z.

[9] Horub KE, Julius T. A mathematical model for the vector transmission and control of Banana Xanthomonas Wilt. *Journal of Mathematics Research*. 2017; 9(4): 101-113. Available from: https://doi.org/10.5539/jmr.v9n4p101.

[10] Nannyonga B, Luboobi LS, Tushemerirwe P, Jabłońska-Sabuka M. Using contaminated tools fuels outbreaks of Banana Xanthomonas Wilt: An optimal control study within plantations using Runge-Kutta fourth-order algorithms. *International Journal of Biomathematics*. 2015; 8(5): 1550065. Available from: https://doi.org/10.1142/S1793524515500655.

[11] Nakakawa J, Mugisha JY, Shaw MW, Tinzaara W, Karamura E. Banana Xanthomonas Wilt infection: The role of debudding and roguing as control options within a mixed cultivar plantation. *International Journal of Mathematics and Mathematical Sciences*. 2017; 2017: 4865015. Available from: https://doi.org/10.1155/2017/4865015.

[12] Nakakawa J, Mugisha JYT, Shaw MW, Karamura E. A mathematical model for the dynamics of Banana Xanthomonas Wilt with vertical transmission and inflorescence infection. *Journal of Biological Systems*. 2016; 24(1): 147-165. Available from: https://doi.org/10.1142/S021833901650008X.

[13] Kweyunga EH, Tumwine JK, Karamura EB. Modeling the dynamics of Banana Xanthomonas Wilt transmission incorporating infectious force in both asymptomatic and symptomatic stages. *Journal of Advances in Mathematics and Computer Science*. 2018; 29(3): 1-17. Available from: https://doi.org/10.9734/JAMCS/2018/44336.

[14] Mapinda JJ, Mwanga GG, Nyerere N, Masanja VG. A mathematical model to assess the role of neglected control techniques in the dynamics of Banana Xanthomonas Wilt disease. *International Journal of Advances in Scientific Research and Engineering*. 2022; 8(1): 107-123. Available from: https://doi.org/10.31695/IJASRE.2022.8.1.12.

[15] Kilbas AA, Srivastava HM, Trujillo JJ. *Theory and applications of fractional differential equations*. Amsterdam:

Elsevier Science; 2006.
[16] Podlubny I. *Fractional differential equations: An introduction to fractional derivatives, fractional differential equations, to methods of their solution and some of their applications*. San Diego: Academic Press; 1999.
[17] Oldham KB, Spanier J. *The fractional calculus theory and applications of differentiation and integration to arbitrary order*. Amsterdam: Elsevier; 1974.
[18] Caputo M, Fabrizio M. A new definition of fractional derivative without singular kernel. *Progress in Fractional Differentiation & Applications*. 2015; 1(2): 73-85. Available from: https://doi.org/10.12785/pfda/010201.
[19] Atangana A, Baleanu D. New fractional derivatives with non-local and non-singular kernel: Theory and application to heat transfer model. *Thermal Science*. 2016; 20(2): 763-769.
[20] Ahmad S, Ullah A, Al-Mdallal QM, Khan H, Shah K, Khan A. Fractional order mathematical modeling of COVID-19 transmission. *Chaos, Solitons & Fractals*. 2020; 139: 110256. Available from: https://doi.org/10.1016/j.chaos.2020.110256.
[21] Rajagopal K, Hasanzadeh N, Parastesh F, Hamarash II, Jafari S, Hussain I. A fractional-order model for the novel coronavirus (COVID-19) outbreak. *Nonlinear Dynamics*. 2020; 101(1): 711-718. Available from: https://doi.org/10.1007/s11071-020-05757-6.
[22] Ma W, Zhao Y, Guo L, Chen Y. Qualitative and quantitative analysis of the COVID-19 pandemic by a two-side fractional-order compartmental model. *ISA Transactions*. 2022; 124: 144-156. Available from: https://doi.org/10.1016/j.isatra.2022.01.008.
[23] Kumar S, Chauhan RP, Momani S, Hadid S. Numerical investigations on COVID-19 model through singular and nonsingular fractional operators. *Numerical Methods for Partial Differential Equations*. 2024; 40(1): e22707. Available from: https://doi.org/10.1002/num.22707.
[24] Khan MA, Ullah S, Kumar S. A robust study on 2019-nCoV outbreaks through non-singular derivative. *The European Physical Journal Plus*. 2021; 136: 168. Available from: https://doi.org/10.1140/epjp/s13360-021-01159-8.
[25] Baleanu D, Mohammadi H, Rezapour S. A fractional differential equation model for the COVID-19 transmission by using the Caputo-Fabrizio derivative. *Advances in Difference Equations*. 2020; 2020: 299. Available from: https://doi.org/10.1186/s13662-020-02762-2.
[26] Sinan M, Shah K, Kumam P, Mahariq I, Ansari KJ, Ahmad Z, et al. Fractional order mathematical modeling of typhoid fever disease. *Results in Physics*. 2022; 32: 105044. Available from: https://doi.org/10.1016/j.rinp.2021.105044.
[27] Vellappandi M, Kumar P, Govindaraj V. Role of fractional derivatives in the mathematical modeling of the transmission of Chlamydia in the United States from 1989 to 2019. *Nonlinear Dynamics*. 2023; 111: 4915-4929. Available from: https://doi.org/10.1007/s11071-022-08073-3.
[28] Zarin R, Khan A, Kumar P. Fractional-order dynamics of Chagas-HIV epidemic model with different fractional operators. *AIMS Mathematics*. 2022; 7(10): 18897-18924. Available from: https://doi.org/10.3934/math.20221041.
[29] Kumar P, Govindaraj V, Erturk VS. A novel mathematical model to describe the transmission dynamics of tooth cavity in the human population. *Chaos, Solitons & Fractals*. 2022; 161: 112370. Available from: https://doi.org/10.1016/j.chaos.2022.112370.
[30] Abbas S, Tyagi S, Kumar P, Ertürk VS, Momani S. Stability and bifurcation analysis of a fractional-order model of cell-to-cell spread of HIV-1 with a discrete time delay. *Mathematical Methods in the Applied Sciences*. 2022; 45(11): 7081-7095. Available from: https://doi.org/10.1002/mma.8226.
[31] Yüzbaşı Ş, Izadi M. Bessel-quasilinearization technique to solve the fractional-order HIV-1 infection of $CD4^+$ T-cells considering the impact of antiviral drug treatment. *Applied Mathematics and Computation*. 2022; 431: 127319. Available from: https://doi.org/10.1016/j.amc.2022.127319.
[32] Etemad S, Avci I, Kumar P, Baleanu D, Rezapour S. Some novel mathematical analysis on the fractal-fractional model of the AH1N1/09 virus and its generalized Caputo-type version. *Chaos, Solitons & Fractals*. 2022; 162: 112511. Available from: https://doi.org/10.1016/j.chaos.2022.112511.
[33] Kumar S, Kumar A, Samet B, Dutta H. A study on fractional host-parasitoid population dynamical model to describe insect species. *Numerical Methods for Partial Differential Equations*. 2021; 37(2): 1673-1692. Available from: https://doi.org/10.1002/num.22603.

[34] Kumar S, Kumar R, Osman MS, Samet B. A wavelet based numerical scheme for fractional order SEIR epidemic of measles by using Genocchi polynomials. *Numerical Methods for Partial Differential Equations*. 2021; 37(2): 1250-1268. Available from: https://doi.org/10.1002/num.22577.

[35] Mohammadi H, Kumar S, Rezapour S, Etemad S. A theoretical study of the Caputo-Fabrizio fractional modeling for hearing loss due to Mumps virus with optimal control. *Chaos, Solitons & Fractals*. 2021; 144: 110668. Available from: https://doi.org/10.1016/j.chaos.2021.110668.

[36] Odibat Z, Baleanu D. Numerical simulation of initial value problems with generalized Caputo-type fractional derivatives. *Applied Numerical Mathematics*. 2020; 156: 94-105. Available from: https://doi.org/10.1016/j.apnum.2020.04.015.

[37] Kumar P, Erturk VS, Kumar A. A new technique to solve generalized Caputo-type fractional differential equations with the example of computer virus model. *Journal of Mathematical Extension*. 2021; 15(12): 1-23. Available from: https://doi.org/10.30495/JME.SI.2021.2052.

[38] Bhalekar S, Daftardar-Gejji V. A predictor-corrector scheme for solving nonlinear delay differential equations of fractional order. *Journal of Fractional Calculus and Applications*. 2011; 1(5): 1-9.

[39] Odibat Z, Erturk VS, Kumar P, Govindaraj V. Dynamics of generalized Caputo type delay fractional differential equations using a modified predictor-corrector scheme. *Physica Scripta*. 2021; 96(12): 125213. Available from: https://doi.org/10.1088/1402-4896/ac2085.

[40] Odibat Z, Erturk VS, Kumar P, Makhlouf AB, Govindaraj V. An implementation of the generalized differential transform scheme for simulating impulsive fractional differential equations. *Mathematical Problems in Engineering*. 2022; 2022: 8280203. Available from: https://doi.org/10.1155/2022/8280203.

[41] Jhinga A, Daftardar-Gejji V. A new finite-difference predictor-corrector method for fractional differential equations. *Applied Mathematics and Computation*. 2018; 336: 418-432. Available from: https://doi.org/10.1016/j.amc.2018.05.003.

[42] Kumar P, Erturk VS, Murillo-Arcila M, Govindaraj V. A new form of L1-predictor-corrector scheme to solve multiple delay-type fractional order systems with the example of a neural network model. *Fractals*. 2023; 31(4): 2340043. Available from: https://doi.org/10.1142/S0218348X23400431.

[43] Mahatekar Y, Scindia PS, Kumar P. A new numerical method to solve fractional differential equations in terms of Caputo-Fabrizio derivatives. *Physica Scripta*. 2023; 98(2): 024001. Available from: https://doi.org/10.1088/1402-4896/acaf1a.

[44] Alikhanov AA. A new difference scheme for the time fractional diffusion equation. *Journal of Computational Physics*. 2015; 280: 424-438. Available from: https://doi.org/10.1016/j.jcp.2014.09.031.

[45] Yan Y, Sun Z-Z, Zhang J. Fast evaluation of the Caputo fractional derivative and its applications to fractional diffusion equations: A second-order scheme. *Communications in Computational Physics*. 2017; 22(4): 1028-1048. Available from: https://doi.org/10.4208/cicp.OA-2017-0019.

[46] Izadi M, Srivastava HM. Fractional clique collocation technique for numerical simulations of fractional-order Brusselator chemical model. *Axioms*. 2022; 11(11): 654. Available from: https://doi.org/10.3390/axioms11110654.

[47] Izadi M, Yüzbaşı Ş, Adel W. Accurate and efficient matrix techniques for solving the fractional LotkaVolterra population model. *Physica A: Statistical Mechanics and its Applications*. 2022; 600: 127558. Available from: https://doi.org/10.1016/j.physa.2022.127558.

[48] Makhlouf AB, El-Hady ES. Novel stability results for Caputo fractional differential equations. *Mathematical Problems in Engineering*. 2021; 2021: 9817668. Available from: https://doi.org/10.1155/2021/9817668.

[49] Langlands TAM, Henry BI. The accuracy and stability of an implicit solution method for the fractional diffusion equation. *Journal of Computational Physics*. 2005; 205(2): 719-736. Available from: https://doi.org/10.1016/j.jcp.2004.11.025.

[50] Sun Z-Z, Wu X. A fully discrete difference scheme for a diffusion-wave system. *Applied Numerical Mathematics*. 2006; 56(2): 193-209. Available from: https://doi.org/10.1016/j.apnum.2005.03.003.

[51] Lin Y, Xu C. Finite difference/spectral approximations for the time-fractional diffusion equation. *Journal of Computational Physics*. 2007; 225(2): 1533-1552. Available from: https://doi.org/10.1016/j.jcp.2007.02.001.